IOSR Journal of Applied Chemistry (IOSR-JAC)
e-ISSN: 2278-5736.Volume 19, Issue 6 Ser. I (June. 2026), PP 20-32
www.iosrjournals.org

Development of Bio-Adsorbent from Nile Perch (*Lates Niloticus*) Scales for Efficient Removal of Heavy Metal Ions from Aqueous Solution

Okpaegbe U.C., Egah, G.O., Hikon B.N and Bako D.B
[1]*Department of Chemistry, Faculty of Physical Sciences, Federal University Wukari, Taraba State, Nigeria*

Abstract
This study investigates the removal of Cr(III) and Ni(II) ions from aqueous solution using chitosan derived from fish scale Lates niloticus (Giwan Ruwa) in a batch adsorption system. Chitosan was prepared from fish scales through deproteinization, demineralization, and deacetylation, and subsequently modified into bead form. The prepared adsorbent was characterized using Fourier Transform Infrared (FTIR) spectroscopy and Scanning Electron Microscopy (SEM) to determine its functional groups and surface morphology. The effects of adsorption parameters such as pH, contact time, adsorbent dosage, temperature, and initial metal ion concentration were investigated. The results showed that adsorption of Cr(III) was favoured at acidic pH, while Ni(II) adsorption was enhanced under alkaline conditions. Adsorption capacity increased with increasing initial concentration and contact time for Ni(II), whereas Cr(III) showed maximum removal at shorter contact times. Temperature studies indicated that Ni(II) adsorption is endothermic while Cr(III) adsorption is exothermic. Kinetic studies revealed that adsorption followed the pseudo-second-order model, indicating chemisorption as the dominant mechanism. Equilibrium data fitted better to the Freundlich isotherm, suggesting heterogeneous multilayer adsorption. The adsorption process was found to be spontaneous for both metals. The results indicate that fish scale chitosan is an effective, low-cost, and environmentally friendly adsorbent for the removal of Cr(III) and Ni(II) ions from aqueous solutions.

Keywords: Adsorption, Chitosan, Kinetic, Isotherm and Thermodynamics

---

Date of Submission: 09-06-2026 Date of Acceptance: 19-06-2026

I. INTRODUCTION

Heavy metal contamination remains one of the most pressing threats to aquatic ecosystems because of their toxicity, persistence, and tendency to bioaccumulate in living organisms. Unlike organic pollutants, heavy metals are non-biodegradable and even at very low concentrations they can pose significant risks to human health and wildlife (Babatunde, and Ibrahim, 2020). Rapid industrial development has intensified the release of these metals into the environment, making them a global environmental concern. Among the commonly reported contaminants in industrial effluents are cadmium, chromium, nickel, lead, mercury, and zinc, which are discharged from operations such as electroplating, mining, smelting, battery and paint manufacturing, tanneries, petroleum refining, pesticide production, and the printing industry (Goci, et al., (2023). Several conventional technologies such as chemical precipitation, ion exchange, electrodialysis, and membrane filtration are used for metal removal. However, these methods are often limited by high operational costs, poor efficiency at low concentrations, and the production of secondary wastes that pose additional treatment problems (Kurniawan et al., 2006; Gavrilescu, 2004; Reddad *et al*., 2002). These drawbacks have encouraged the exploration of cost-effective, sustainable, and eco-friendly alternatives. In recent years, biomaterials have attracted significant attention in metal removal research due to their eco-friendly properties and wide applicability in pollution control. Fish scales, an abundant waste product in many Nigerian communities, provide a renewable source of chitin that can be converted to chitosan and modified into functional adsorbents (Ali, *et al*., 2024). However, little research has been carried out on the use of chitosan from *Lates niloticus* (Giwan Ruwa) fish scales for the removal of Cr(III) and Ni(II) ions (Goci, et al., 2023; Jabeen, et al., 2022; Kurita, 2020; Karthik et al., 2022; Mahmoud et al., 2023; N'diaye et al., 2022; Ngah & Fatinathan, 2010; Rinaudo, 2018 and Yadav et al., 2019) . This research is aimed at investigating the removal of Cr(III) and Ni(II) ions from aqueous solution using chitosan and its derivatives prepared from the scales of *Lates niloticus* (Giwan Ruwa).

II. Adsorption Isotherms

2.1. Freundlich Isotherm

The Freundlich isotherm model assumes that the removal of metal ions occurs on a heterogeneous adsorbent surface and can be applied to multilayer adsorption. It can also be used for both mono-layer and multi-layer adsorption. Linear equation of Freundlich isotherm was adopted by Okpaegbe et al., (2021). This is given as Equation 1.

$$logQ_e = \frac{1}{n} logc_e + logK_f \quad (1)$$

where Qe (mg/g) is the amount of adsorbate adsorbed per unit mass and Ce (mg/L) is the equilibrium concentration. K_F is the Freundlich constant and 1/n is a function of the strength of adsorption.

2.2. Langmuir Isotherm

This is applied to monolayer adsorption on surface containing a finite number of identical binding sites. The Langmuir adsorption model is expressed as shown in Equation 2.

$$\frac{1}{Qe} = \frac{1}{Q_m} + \frac{1}{C_e} \times \frac{1}{bQ_m} \quad (2)$$

where Q_m (mg/g) is the monolayer sorption capacity indicating the total number of binding sites available for sorption, C_e is the equilibrium concentration of the solute (mg/L), Q_e (mg/g) is the amount of solute sorbed per unit mass and b (L/mg) is the Langmuir constant for the adsorbate-adsorbent. The percentage of metal ions removed was obtained using the Equation 3.

$$\% \text{ Removal} = \frac{C_0 - C_e}{C_0} \times 100 \quad (3)$$

Where %R is the percentage of Cr or Ni ions removed before and after adsorption (Rinaudo, 2018).

2.3. Adsorption Kinetics Studies

Chemical kinetics is a method used to determine how experimental conditions affect the rate of chemical reaction. Pseudo-first-order and pseudo-second-order kinetic models were used to analyze the experimental data and model of the adsorption processes.

2.3.1 Pseudo-First Order Model

The Pseudo-First Order Kinetic Model was used to predict the adsorption kinetics of Cr and Ni. The model is expressed as in equation 4:

$$\log(\text{qe} - \text{qt}) = \log \text{qe} - \frac{K_1}{2.303} \times t \quad (4)$$

Where K_1 (min^{-1}) is the rate constant of the Pseudo-first order adsorption, qt (mg/g) is the amount of adsorption at time t (min), and qe (mg/g) is the amount of adsorption at equilibrium. By plotting log(qe - qt) versus t, the adsorption rate was calculated (Mahmoud et al., 2023).

2.3.2. Pseudo-Second Order Model

The adsorption kinetic data were also analyzed using the Pseudo-Second Order Model expressed as Equation 5.

$$\frac{t}{Q_t} = \frac{1}{K_2 - Qe^2} + \frac{t}{Q_e} \quad 5$$

Where K_2 is the pseudo-second order rate constant. Integration of the equation with conditions qt = 0 at t = 0 and qe = qt at t = t gives a linear relationship from which qe and K_2 were evaluated (Ali et al., 2024).

2.4. Adsorption Thermodynamics

In thermodynamic studies, the equilibrium constant (K) and its dependence on temperature were used to predict the thermodynamic parameters, including changes in Gibbs free energy (ΔG°), enthalpy (ΔH°), and entropy (ΔS°) associated with the adsorption of Cr and Ni ions. These parameters were determined by applying Equations 6.

$$\Delta G° = -RT \ln K \quad (6)$$

Where K = Langmuir constant, T = Absolute temperature (K), and R = Universal gas constant (8.314 $J \cdot mol^{-1} \cdot K^{-1}$). The plot of ln K as a function of 1/T yields a straight line, from which ΔH° and ΔS° were calculated from the slope and intercept, respectively.

III. MATERIALS AND METHODS

3.1 Methods

3.1.1 Sample Collection and Preparation

Fish scales were obtained as waste materials from fish vendors at the Wukari Fish Market, Taraba State, Nigeria. The collected scales were thoroughly washed with tap water to remove adhering impurities and debris,

followed by rinsing with distilled water to ensure complete cleanliness. The cleaned samples were then air-dried at room temperature and subsequently oven-dried at 100 °C to eliminate residual moisture. The dried scales were cut into smaller pieces using sterilized scissors and pulverized using a clean mortar and pestle to obtain a fine powder. The powdered sample was then sieved through a 2 mm mesh to achieve uniform particle size. The processed material was stored in an airtight container until further use to prevent contamination and moisture absorption.

3.1.2 Isolation of Chitin from Fish Scales

Isolation of chitin was achieved by two major steps: deproteinization and demineralization, as described by Okpaegbe et al., (2021).

- Deproteinization: 5 g of ground fish scales were weighed into conical flasks, and 100 mL of 5% NaOH solution was added. The mixture was boiled and stirred at 100 °C for 2 hours in a water bath. The residue was collected on a sintered glass funnel, washed with distilled water to neutral pH (7.0), and oven-dried to constant weight at 100 °C.
- Demineralization: 1 g of the deproteinized residue was treated with 20 mL of 5% HCl at room temperature under continuous mixing for 18 hours to dissolve calcium carbonate. The crude chitin was washed with double distilled water to pH 7.0 and dried at 100 °C to constant weight.

3.1.3 Preparation of Swollen Chitosan Beads

Swollen beads were obtained by dissolving 2 g of chitosan flakes in 60 ml of 5% (v/v) acetic acid at room temperature under continuous stirring for 24 hours. The 5% acetic acid solution was prepared by diluting 60 ml of acetic acid in 1200 ml of distilled water. Similarly, 40 g of chitosan flakes from the ground fish scales were dissolved in 60 ml of 5% acetic acid solution with continuous stirring at room temperature. The thick solution was kept overnight and subsequently introduced dropwise into 500 ml of 0.5 mol/L NaOH solution while stirring. The formed beads were allowed to remain in the alkaline medium for about 30 minutes to neutralize residual acetic acid. They were then collected by filtration, rinsed thoroughly with distilled water, and air-dried. Finally, the beads were ground and sieved to obtain a uniform particle size below 200 µm before undergoing further modification.

3.2. Preparation of Stock Solutions of Cr and Ni

A stock solution of 25 mg/L of chromium was prepared by dissolving an appropriate amount of potassium dichromate ($K_2Cr_2O_7$) in distilled water using a 1000 ml volumetric flask. In the same way, a 25 mg/L stock solution of nickel was prepared by dissolving nickel nitrate hexahydrate ($Ni(NO_3)_2 \cdot 6H_2O$) in distilled water and making up to the 1000 ml mark in a volumetric flask. The pH of both solutions was adjusted as necessary using sodium hydroxide or hydrochloric acid (Ali et al., 2024).

3.3. Batch Adsorption Experiments

Batch mode adsorption experiments were conducted in 250 ml Erlenmeyer flasks to determine the best operating conditions that would facilitate the adsorption of Cr and Ni ions onto the adsorbent (Okpaegbe et al., 2021).

3.3.1. Effect of Adsorbent Dosage

The effect of adsorbent dosage on the removal of Cr(III) and Ni(II) ions was studied by varying the mass of Nile perch (*Lates niloticus*) fish scale adsorbent while keeping other experimental parameters constant. Batch adsorption experiments were carried out in 250 mL Erlenmeyer flasks containing 25 mL of metal ion solution at an initial concentration of 50 mg/L. Different masses of the adsorbent (0.01, 0.02, 0.05, 0.10, and 0.20 g) were added to each flask. The pH of the solutions was adjusted to the optimum value (pH 7.0) using 1 M HCl or 1 M NaOH. The mixtures were agitated at 150 rpm for 1 hour at 30 °C, and then filtered through 0.45 µm Whatman filter paper. The equilibrium concentrations of Cr(III) and Ni(II) were determined using Atomic Absorption Spectroscopy (AAS).

3.3.2. Effect of Contact Time

Experiments were carried out to determine the contact time needed by the system to reach equilibrium. From the stock solutions, 0.1 g each of the adsorbents (chitosan and modified chitosans) were added. The pH was then adjusted to 6.0 using 1M HCl or 1M NaOH and agitated in a rotary mixer at various times at room temperature. After each time of agitation, the samples were filtered through 0.45 µm cellulose filter paper, and the concentration of the metals remaining in the aqueous solution was determined using AAS. The metal uptake q (mg ion metal/g sorbent) was determined using Equation 7.

$$q = (C_0 - C_e) \times \frac{V}{m} \quad (7)$$

Where Co and Ce are the initial and final metal ion concentrations (mg/L), respectively, V is the volume of solution (ml), and m is the adsorbent weight (g) in dry form.

IV. RESULTS

4.1 Characterization of Fish Scale Chitosan Adsorbent

4.1.1 Fourier Transform Infrared (FTIR) Spectroscopy

The FTIR spectra of the prepared fish scale chitosan adsorbent before adsorption of Cr(III) and Ni(II) ions are presented in Figure 1. The corresponding peak assignments are summarized in Tables 1. Figure 1 shows the FTIR spectrum of fish scale chitosan adsorbent (FSCA) before adsorption. The FTIR analysis of FSCA in the 3200–4000 cm^{-1} frequency range shows the band at 3,357.00 cm^{-1} which appeared broadened and shifted, confirming that the O–H and N–H groups were involved in metal ion binding. Similarly, the C–N stretching band at ~1411.00 cm^{-1} showed a noticeable shift after adsorption, confirming that the amino groups ($–NH_2$) served as active sites for the complexation of Cr(III) and Ni(II) ions onto the surface of the fish scale chitosan adsorbent (Chowdhury and Saha, 2013).

Table 1: FTIR Analysis of Fish Scale Chitosan Adsorbent Before Adsorption

Group Freq. (cm^{-1})	Functional Groups	Observed Frequency (cm^{-1}) FSCA	Assignment
4000–3200	Alcohol / Amine	3357.00 (shifted/broadened)	O–H and N–H stretch
3200–2800	Alkanes	2789.00	C–H stretch
1800–1600	Amide II	1625.00 (shifted)	N–H bending / C=O stretch
1600–1400	Amine	1411.00 (shifted)	C–N stretch
1200–1000	Polysaccharide	1082.00	C–O–C stretch (pyranose ring)
1000–800	Saccharide	926.00	Saccharide structure

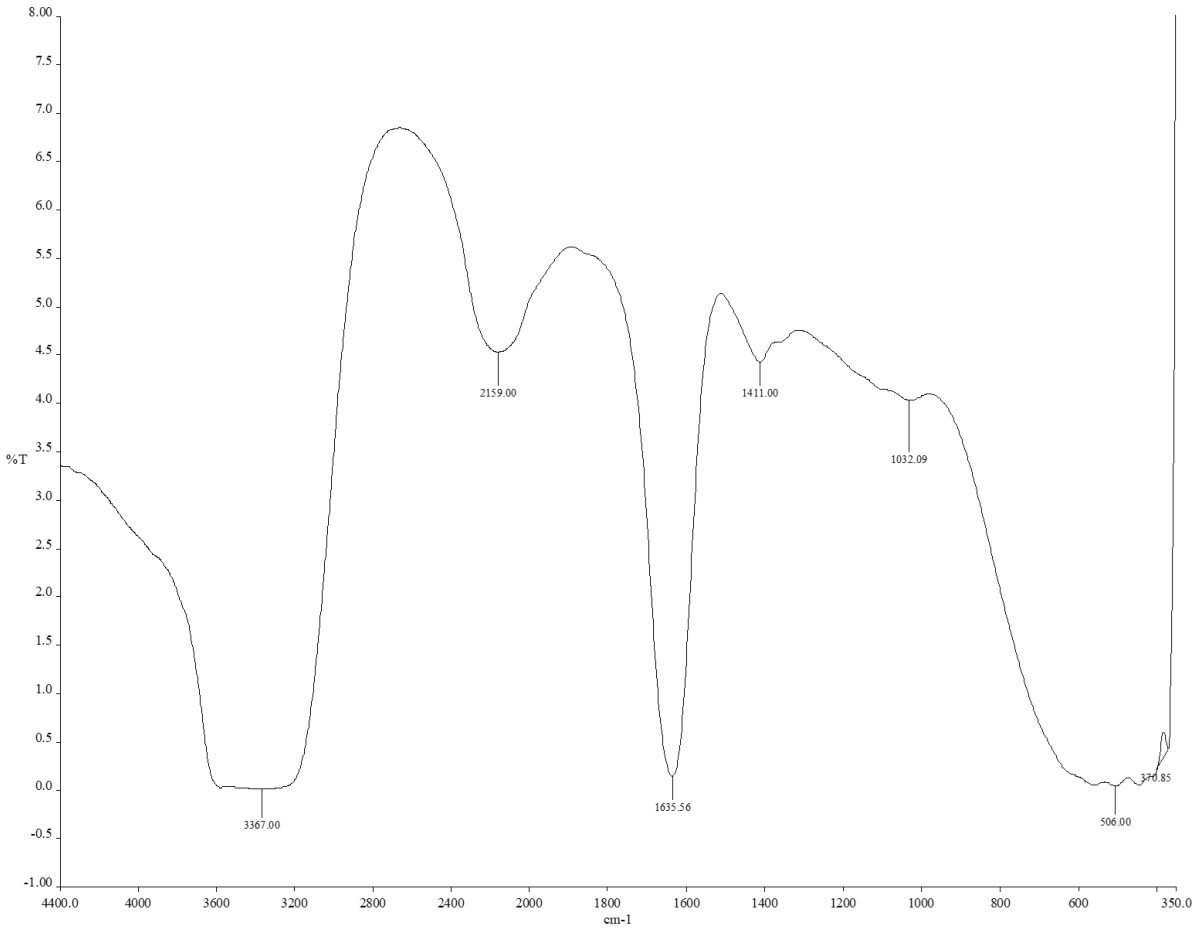

Figure 1: FTIR Spectrum of Fish Scale Chitosan Adsorbent (FSAA) After Adsorption

4.1.2 Scanning Electron Microscopy (SEM)

The surface morphology of the fish scale chitosan adsorbent before adsorption is shown in Plate 1. The SEM micrograph was obtained at 12,000× magnification, 15 kV high voltage, 11.6 mm working distance, and 70 Pa

chamber pressure. SEM result shows the pore development and occupation by adsorbates (Naswir et al., 2013). The morphological analysis of the surface of the chitosan adsorbent reveals that the adsorbent is highly irregular, rough, and porous with visible cracks and folded lamellar formations, which enables it to trap the adsorbate, indicating its good adsorption properties. The high surface roughness and porosity of the adsorbent make it a suitable and effective material for the removal of Cr(III) and Ni(II) ions from aqueous solution (Karthik et al., 2022)

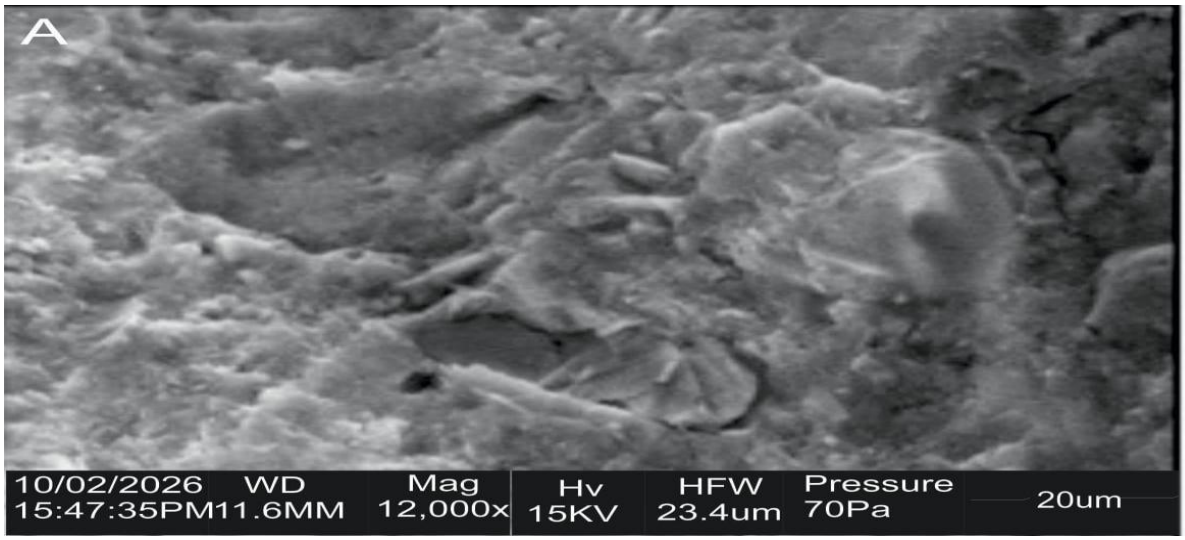

4.2. Batch Adsorption Experiment

4.2.1. Effect of Initial Solution pH on Adsorption of Cr(III) and Ni(II)

The result in Figure 2 shows the effect of pH on the adsorption of Cr(III) and Ni(II) with an initial concentration of 50 mg/L. The highest percentage removal for Cr(III) was observed at pH 3 (97.482%) and the lowest at pH 9 (94.842%), indicating that Cr(III) adsorption is favoured under acidic conditions. For Ni(II), the highest percentage removal is at pH 11 (99.1%) and the lowest is at pH 3 (98.04%), indicating that Ni(II) adsorption is favoured under alkaline conditions. The pH-dependent behaviour of these two metals reflects their distinct ionic speciation in solution. Cr(III) exists primarily as negatively charged chromate ($HCrO_4^-$) and dichromate ($Cr_2O_7^{2-}$) anions, which are electrostatically attracted to the protonated amino groups ($-NH_3^+$) of chitosan at low pH, resulting in high Cr(III) removal under acidic conditions (Gupta *et al*., 2016). At higher pH values, the adsorbent surface becomes less positively charged, reducing this electrostatic attraction and thereby decreasing Cr(III) removal efficiency. For Ni(II), the increase in adsorption with pH is attributed to the deprotonation of amino groups at higher pH, which reduces competition from H^+ ions for surface binding sites and enhances complexation of Ni(II) cations with $-NH_2$ groups (Mousavi and Seyedi, 2021). From this study, the fish scale chitosan adsorbent adsorbs Ni(II) more efficiently under alkaline conditions and Cr(III) more efficiently under acidic conditions. According to Babatunde and Ibrahim (2020), similar opposing pH trends were observed for heavy metals on activated adsorbent materials.

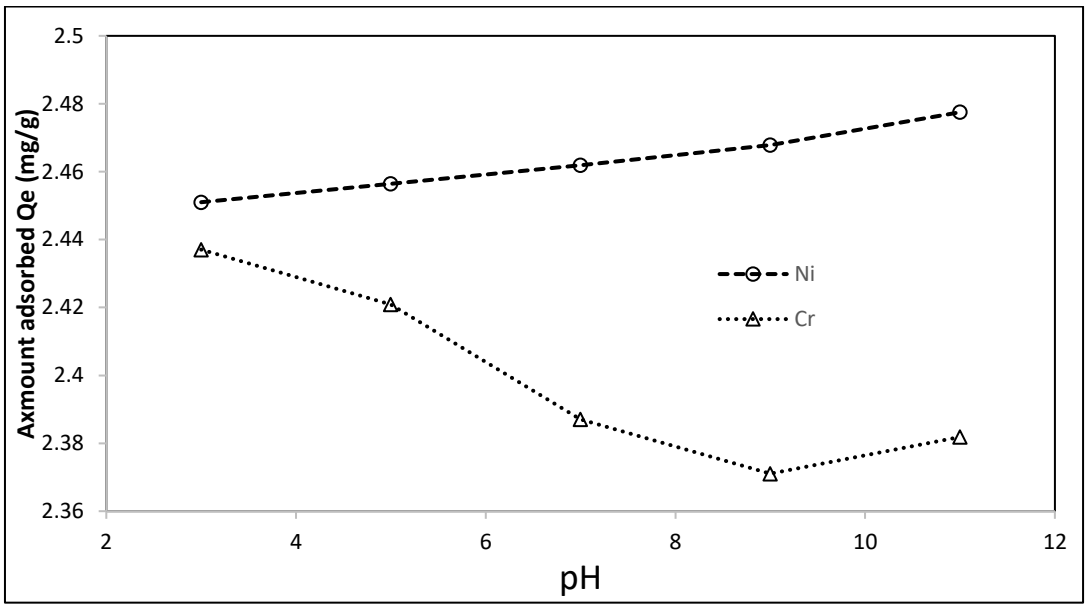

Figure 2: Effect of pH on Adsorption of Cr(III) and Ni(II) by Fish Scale Chitosan Adsorbent

4.2.2. Effect of Temperature on Adsorption of Cr(III) and Ni(II)

The result in Figure 3 shows that for Ni(II), adsorption capacity increases with increase in temperature from 2.4513 mg/g at 303 K to 2.4603 mg/g at 343 K, with percentage removal rising from 98.052% to 98.412%. This indicates that the adsorption of Ni(II) onto fish scale chitosan is endothermic in nature, and temperature favours the process. For Cr(III), the adsorption capacity decreased from 2.43625 mg/g at 303 K to 2.41875 mg/g at 343 K, with percentage removal declining from 97.45% to 96.75%, indicating that increase in temperature results in decrease in adsorption (Karthik et al., 2022). The percentage removal of Ni(II) using fish scale chitosan adsorbent is higher than that of Cr(VI) across all temperature values, which shows that fish scale chitosan adsorbent adsorbs Ni(II) more than Cr(III) when subjected to varying temperatures. Temperature at 343 K (70 °C) was the most favourable for Ni(II) adsorption, while 303 K (30 °C) was most favourable for Cr(III) adsorption.

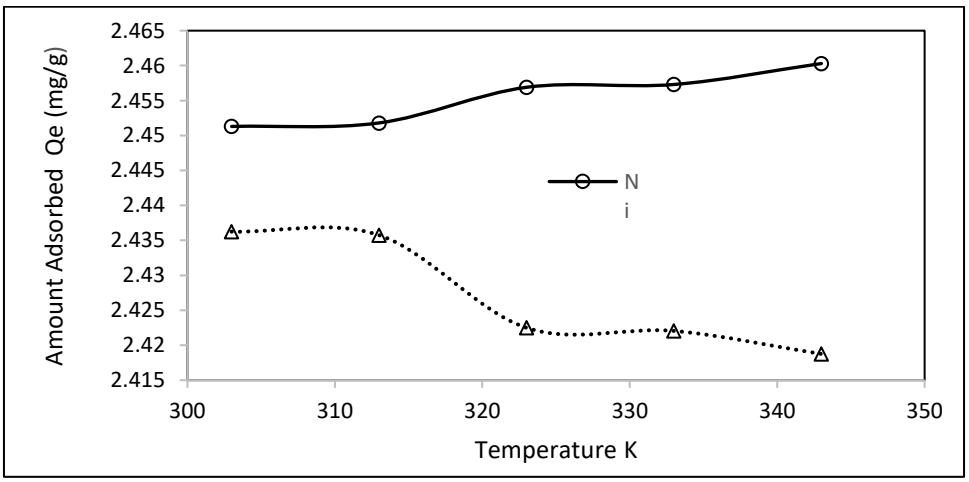

Figure 3: Effect of Temperature on Adsorption of Cr(III) and Ni(II) by Fish Scale Chitosan Adsorbent

4.2.3. Effect of Contact Time on Adsorption of Cr(III) and Ni(II)

The result in Figure 4 (Effect of contact time) shows that for Ni(II), percentage removal increases progressively with increase in contact time, rising from 98.046% at 10 minutes to 98.64% at 60 minutes. The equilibrium contact time for Ni(II) adsorption was reached at 60 minutes, consistent with findings reported by Okpaegbe et al. (2021) who observed a similar equilibrium time for metal ion adsorption using chitosan from Lates niloticus fish scales. The adsorption of Ni(II) on fish scale chitosan increases with contact time because initially there are many empty binding sites available on the adsorbent surface; as contact time increases, these

sites gradually become occupied until equilibrium is reached, after which no more adsorption occurs for Cr(III), the percentage removal showed a decrease with increasing contact time, from 97.7% at 10 minutes to 95.52% at 60 minutes. The adsorption of Cr(III) was highest at 10 minutes, which may be considered the optimum contact time for Cr(III) in this system. This unusual trend for Cr(III) may be attributed to the partial reduction of Cr(III) to Cr(VI) over time and subsequent re-release into solution, or to competitive desorption at longer contact times (Gupta et al., 2016). The adsorption of Ni(II) using fish scale chitosan adsorbent when subjected to varying contact time shows that the percentage removal for Ni(II) is higher than that of Cr(III), which means that the fish scale chitosan adsorbent adsorbs Ni(II) more effectively than Cr(III) across all contact time values studied.

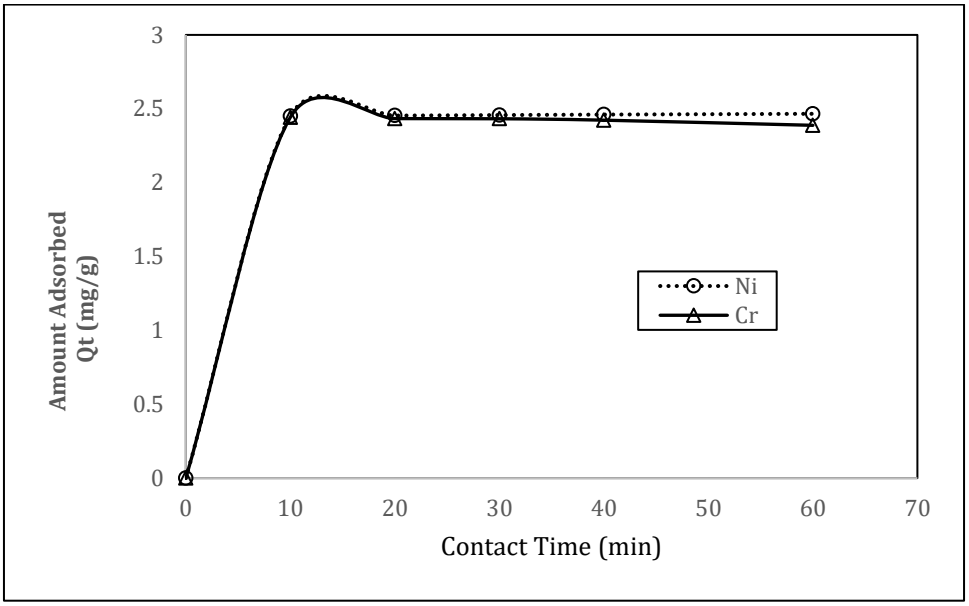

Figure 4: Effect of Contact Time on Adsorption of Cr(III) and Ni(II) by Fish Scale Chitosan Adsorbent

4.2.4. Effect of Adsorbent Dose on Adsorption of Cr(III) and Ni(II)

From the result shown in Figure 5 for adsorbent doseage, it was observed that the adsorption capacity per gram (Qe) decreases for both Cr(III) and Ni(II) with an increase in adsorbent dosage from 0.5 g to 2.5 g. The solution with an initial concentration of 50 mg/L was treated with different amounts of adsorbent ranging from 0.5, 1.0, 1.5, 2.0, and 2.5 g. It was observed that the highest adsorption capacity per gram was recorded at the lowest dose of 0.5 g, with Ni(II) giving 4.9318 mg/g and Cr(III) giving 4.7758 mg/g. The percentage removal of Ni(II) at 0.5 g was 98.636%, while that of Cr(VI) was 95.516%. The percentage removal for both metals remained high across all doses, with Ni(II) consistently showing slightly higher removal than Cr(III). The metal ions uptake per unit mass decreased with increase in adsorbent dosage for both metals. Ahmedna et al., (2000), attributed this to the fact that at high adsorbent dosages, the available metal ions are not sufficient to cover all the exchangeable sites on the biosorbent, resulting in low metal uptake per gram. Maximum uptake per gram was observed at the lowest dosage of 0.5 g for both metals.

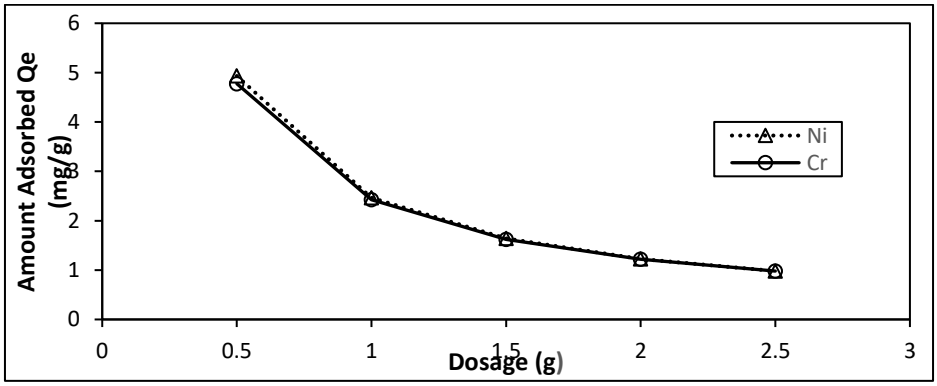

Figure 5: Effect of Adsorbent Dose on Adsorption of Cr(III) and Ni(II) by Fish Scale Chitosan Adsorbent

4.2.5. Effect of Initial Concentration on Adsorption of Cr(III) and Ni(II)

From the result shown in Figure 6, it was observed that adsorption capacity increases with increase in initial metal ion concentration, varying from 50, 100, 150, 200, and 250 mg/L. The amount of Ni(II) adsorbed in mg/g increased from 2.4728 to 12.4519 mg/g, and that of Cr(III) increased from 2.45725 to 12.3835 mg/g across the concentration range studied. This behaviour is attributed to the increased concentration gradient between the bulk solution and the adsorbent surface at higher initial concentrations, which acts as a greater driving force for mass transfer of metal ions to the adsorbent surface (Foo and Hameed, 2010).

The percentage removal of both Ni(II) and Cr(III) remained exceptionally high across all concentration levels, indicating that the fish scale chitosan adsorbent was not saturated within the concentration range tested. The percentage removal for Ni(II) was consistently higher than that for Cr(III) across all concentration levels. The percentage removal for both Ni(II) and Cr(III) using fish scale chitosan when subjected to initial solution concentration shows that the amounts adsorbed for both metals are approximately equal in magnitude, with only minimal differences between them. This is consistent with the behaviour observed by Okpaegbe et al. (2021) for the adsorption of Cd(II) and Mn(II) using chitosan from Lates niloticus , who also observed that adsorption capacity increased significantly with increasing initial concentration.

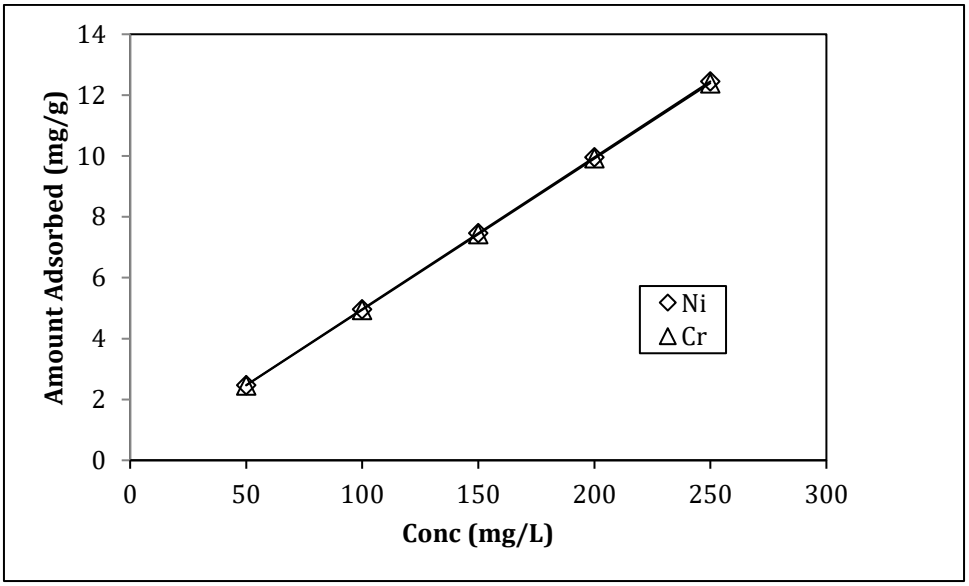

Figure 6: Effect of Initial Concentration on Adsorption of Cr(III) and Ni(II) by Fish Scale Chitosan Adsorbent

4.3. Adsorption Kinetic Model

The experimental data for adsorption of Cr(III) and Ni(II) as a function of time with fish scale chitosan adsorbent were plotted into the form of Lagergren pseudo-first order and Blanchard pseudo-second order kinetic models. The plots are shown in Figures 7 and 8. The results show that the experimental data best fits into the Blanchard pseudo-second order than the Lagergren pseudo-first order for Ni(II), while Cr(III) also showed a better fit to the pseudo-second order model. The experimental data for adsorption of Cr(III) and Ni(II) as a function of contact time with the fish scale chitosan adsorbent were plotted into the form of Lagergren pseudo-first order and Blanchard pseudo-second order kinetic models. The plots are shown in Figures 7 and 8. Their parameters were shown in Table 8. From the correlation coefficients R^2 calculated from the kinetic plots, the pseudo-second order model gave a perfect fit for Nickel with $R^2 = 1$, and for Chromium with $R^2 = 0.9999$, showing that the plot best fits into the Blanchard pseudo-second order kinetic model rather than the Lagergren pseudo-first order of 0.0013 and 0.8616 respectfully suggesting that chemisorption is the rate-limiting step in the adsorption of Cr(III) and Ni(II) onto fish scale chitosan adsorbent, likely involving sharing or exchange of electrons between the metal ions and the $–NH_2$ functional groups of chitosan (Chowdhury and Saha, 2013). These results are similar to the findings of Eze et al., (2020) who observed pseudo-second order behaviour for the adsorption of Cd and Pb on rice husk activated carbon, with $R^2 = 1$ for both metals.

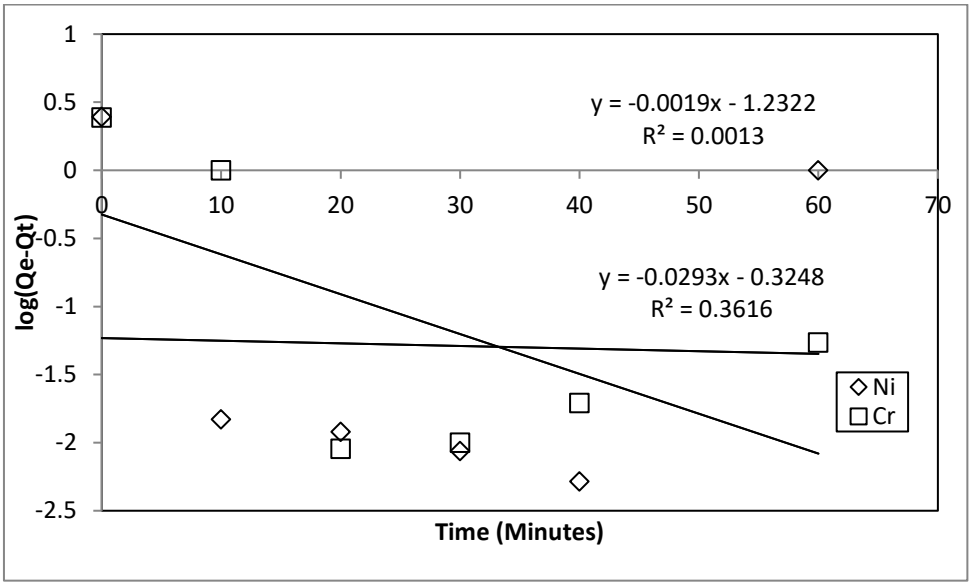

Figure 7: Graph of Lagergren Pseudo-First Order for Cr(III) and Ni(II) Adsorption

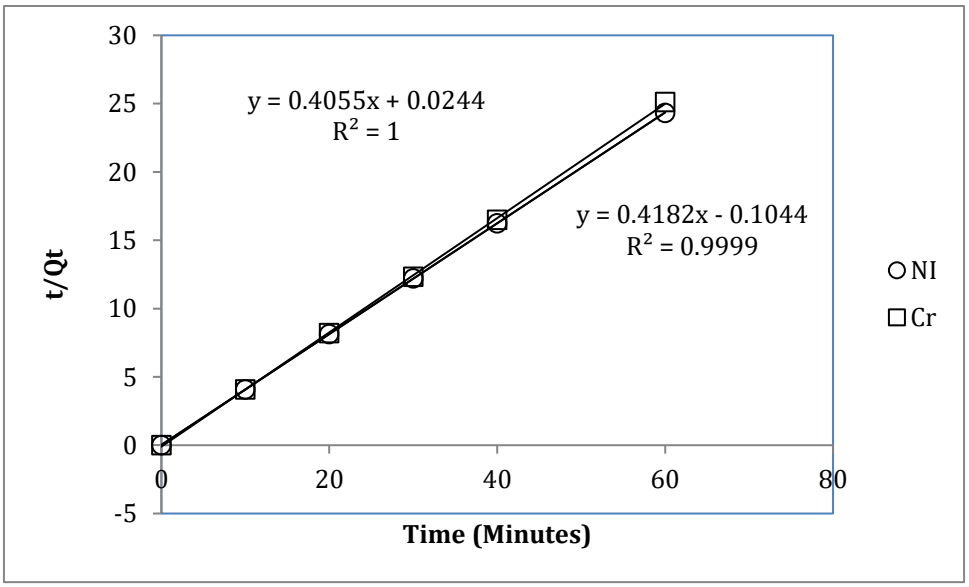

Figure 8: Graph of Blanchard Pseudo-Second Order for Cr(III) and Ni(II) Adsorption

Table 8: Kinetic Parameters for Adsorption Lagergren Pseudo-First Order and Blanchard Pseudo-Second Order for Ni(II) and Cr(III)

Adsorbate	Model	Adsorbent	Parameter	Value
Nickel	First Order	FSCA	K_1 (L min^{-1})	-0.0043
			Qe (mg/g)	0.0586
			R^2	0.0013
Nickel	Second Order	FSCA	K_2 (L min^{-1})	1.0239×10^{-3}
			Qe (mg/g)	0.0002
			R^2	1
Chromium	First Order	FSCA	K_1 (L min^{-1})	0.0674
			Qe (mg/g)	0.4734

			R^2	0.8616
Chromium	Second Order	FSCA	K_2 (L min^{-1})	1.6753
			Qe (mg/g)	2.3912
			R^2	0.9999

4.4. Adsorption Isotherm Models for Adsorption of Cr(III) and Ni(II)

The Langmuir model is based on monolayer adsorption on homogeneous active sites of the adsorbent (Nanganoa et al., 2014). The Langmuir theoretical constants Qm and b were calculated from the slope and intercept of a linear plot of 1/Qe versus 1/Ce. From the results in Figures 9a-b annd Table 9, for Ni(II), the maximum adsorption capacity Qm was found to be 2.6911 mg/g for FSCA, with a Langmuir constant b = 0.1502 L/mg and R^2 = 0.9182, and separation factor R^L = 0.8694. For Cr(III), the Qm was found to be 0.5744 mg/g with b = 0.6842 L/mg and R^2 = 0.5937. The relatively lower R^2 value for Cr(III) (0.5937) compared to Ni(II) (0.9182) suggests that the Langmuir model described Ni(II) adsorption better than Cr(III) adsorption. The R_L values less than 1 indicate that adsorption is favourable for Ni(II) in this system (Krishna and Swamy, 2012). The Freundlich model is governed by heterogeneous adsorption. A plot of log Qe against log Ce was used to determine the Freundlich constants Ko and n. From Table 9, Ni(II) gave Ko = 0.0669 mg/g(L/mg)1/n, n_o = 0.3563, and R^2 = 0.9587. For Cr(III), Ko = 0.2443 mg/g(L/mg)1/n, n_o = 0.1612, and R^2 = 0.8437. From the correlation coefficients R^2, the experimental data for both metals fitted well into the Freundlich isotherm, with Ni(II) showing a higher R^2 of 0.9587 compared to Cr(III) at 0.8437. The higher Freundlich R^2 values compared to the Langmuir values for Cr(III) indicate that the Freundlich model better describes Cr(III) adsorption, confirming heterogeneous multilayer adsorption for Cr(III) on the fish scale chitosan surface. The higher values of n_o for both metals, being less than 1, reflects the heterogeneous nature of the adsorbent surface and is indicative of favourable adsorption conditions (Khalid et al., 2000).

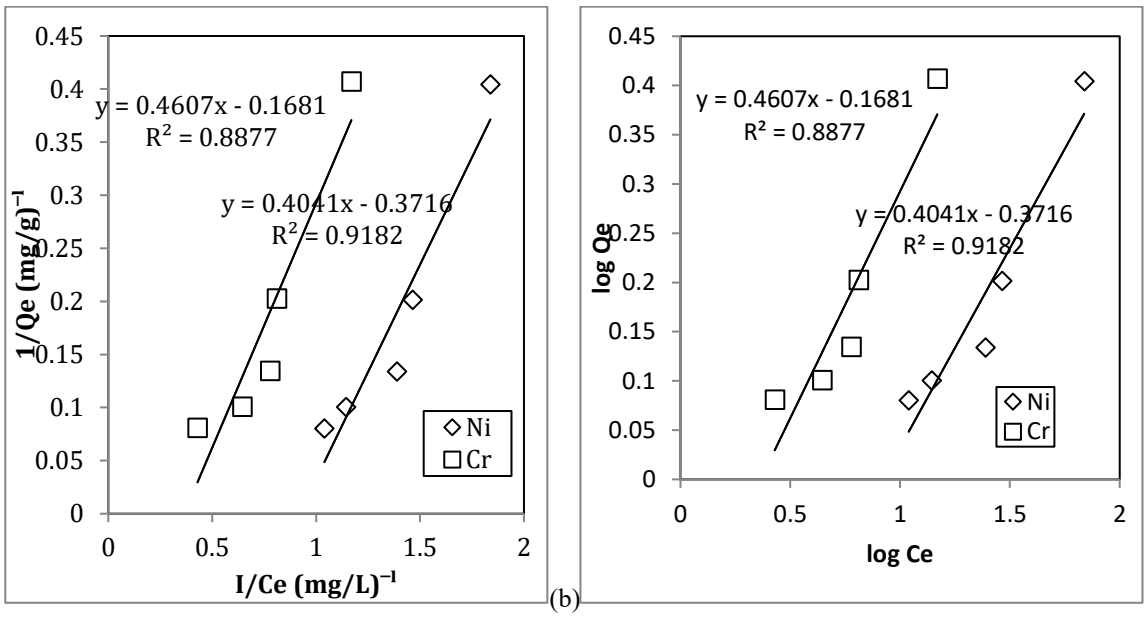

(a) (b)

Figure 9: (a)Freundlich (b) Langmuir Isotherm for Cr(III) and Ni(II) Adsorption on Fish Scale Chitosan Adsorbent (FSCA)

Table 9: Isotherm Parameters for Ni(II) and Cr(III) Adsorption on Fish Scale Chitosan Adsorbent (FSCA)

Adsorbate	Model	Adsorbent	Parameter	Value
Nickel	Freundlich	FSCA	no	0.3563
			R^2	0.9587
			Ko (mg/g)$(L/mg)^{1/n}$	0.0669

Nickel	Langmuir	FSCA	Qm (mg/g)	2.6911
			b (L/mg)	0.1502
			R^2	0.9182
			R^L	0.8694
Chromium	Freundlich	FSCA	no	0.1612
			R^2	0.8437
			Ko (mg/g)(L/mg)$^{1/n}$	0.2443
Chromium	Langmuir	FSCA	Qm (mg/g)	0.5744
			b (L/mg)	0.6842
			R^2	0.8877
			R^L	0.5937

4.5. Thermodynamic Parameters for Adsorption of Cr(III) and Ni(II) by Fish Scale Chitosan Adsorbent

Thermodynamics is an important parameter that determines the spontaneity of the adsorption process (Tan et al., 2012). Table 10 shows the calculated values of thermodynamic parameters for Gibbs free energy change (ΔG°), enthalpy change (ΔH°), and entropy (ΔS°). Results in Table 10 showed the calculated values of thermodynamic parameters. From the table, the value of ΔH° for Ni(II) was calculated to be +4851.4521 kJ/mol, indicating an endothermic adsorption process for Ni(II), meaning that adsorption is favoured by increasing temperature. The positive value of ΔS° for Ni(II) (+22.8962 J/mol•K) suggests an increase in randomness at the solid–liquid interface during adsorption, which may be attributed to the displacement of coordinated water molecules from the Ni(II) ion surface upon binding to the chitosan adsorbent (Mahamallik et al., 2021). For Cr(III), the value of ΔH° was found to be −6065.8146 kJ/mol, indicating an exothermic adsorption process, consistent with the observed decrease in Cr(III) removal at higher temperatures. The negative value of ΔS° for Cr(III) (−18.8971 J/mol•K) indicates a decrease in disorder at the solid–liquid interface during Cr(III) adsorption, suggesting a more ordered arrangement of Cr(III) species on the adsorbent surface (Tan et al., 2012). The negative values of ΔG° for both Ni(II) (−3201.7814 kJ/mol) and Cr(III) (−845.4471 kJ/mol) indicate that the adsorption of both metals was spontaneous under the experimental conditions (Dula et al., 2014).

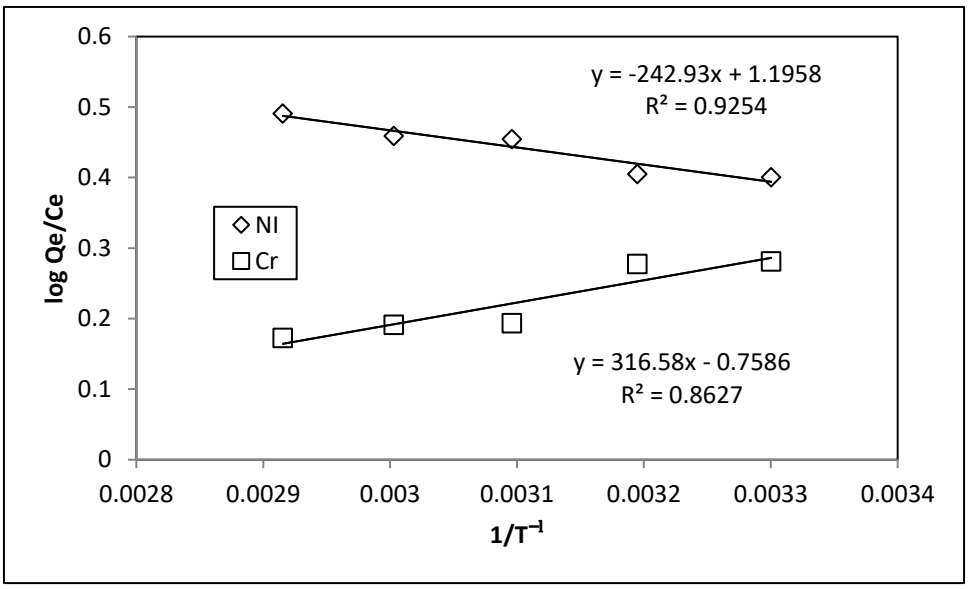

Figure 10: Thermodynamic plot for Adsorption of Cr(III) and Ni(II) by Fish Scale Chitosan Adsorbent

Table 10: Thermodynamic Parameters for Adsorption of Ni(II) and Cr(III) by Fish Scale Chitosan Adsorbent

Adsorbate	Adsorbent	ΔH (kJ/mol·1000)	ΔS (J/mol·K)	R^2	ΔG (kJ/mol·1000)
Nickel	FSCA	4851.4521	22.8962	0.9254	−3201.7814
Chromium	FSCA	−6065.8146	−18.8971	0.8627	−845.4471

V. CONCLUSION

Based on this investigation, it could be concluded that the adsorption characteristics of Cr(III) and Ni(II) onto fish scale are strongly affected by initial solution pH, initial metal ion concentration, adsorbent dosage, temperature, and contact time. The optimum pH for adsorption of Ni(II) was found to be pH 11, while for Cr(III) it was pH_3. The experimental kinetic data for both Cr(III) and Ni(II) were found to fit better into the Blanchard pseudo-second order model than the Lagergren pseudo-first order model, suggesting that chemisorption dominates the rate-limiting step. The equilibrium data for both metals fitted better into the linearized Freundlich isotherm than the Langmuir isotherm, indicating multilayer adsorption. The negative ΔG° values confirmed that the adsorption of both Cr(III) and Ni(II) was spontaneous under all experimental conditions. Above all, fish scale chitosan adsorbent derived from *Lates niloticus* is highly effective, low-cost, biodegradable, and environmentally friendly biosorbent capable of removing Cr(III) and Ni(II) ions from aqueous solutions.

REFERENCES

[1]. Ali, G., Sharma, M., Salama, E. S., Ling, Z., & Li, X. (2024). Applications of chitin and chitosan as natural biopolymer: potential sources, pretreatments, and degradation pathways. *Biomass Conversion and Biorefinery*, *14*(4), 4567-4581.

[2]. Ahmedna, M., Marshall, W. E., Husseiny, A. A., Rao, R. M., & Goktepe, I. (2000). The use of nutshell carbons in drinking water filters for removal of trace metals. Water Research, 34(10), 2813–2819.

[3]. Babatunde, E. O., & Ibrahim, A. A. (2020). Adsorption of lead and cadmium from aqueous solution using activated rice husk: Effect of pH and adsorbent dose. *Journal of Applied Chemistry, 13(2), 45–58.*

[4]. Chowdhury, S., & Saha, P. (2013). Adsorption of crystal violet from aqueous solutions by chemically modified chitosan beads. Environmental Progress & Sustainable Energy, 32(4), 1169–1183.

[5]. Dula, T., Siraj, K., & Kitte, S. A. (2014). Adsorption of hexavalent chromium from aqueous solution using chemically activated carbon prepared from locally available waste of bamboo (Oxytenanthera abyssinica). ISRN Environmental Chemistry, 2014, 1–10.

[6]. Eze, C. N., Eze, V. H. U., & Nweze, C. C. (2020). Heavy metal contamination of water resources and its health implications in southeastern Nigeria. I*nternational Journal of Environmental Pollution and Remediation,* 8(1), 1–12.

[7]. Foo, K. Y., & Hameed, B. H. (2010). Insights into the modeling of adsorption isotherm systems. Chemical Engineering Journal, 156(1), 2–10.

[8]. Gavrilescu, M. (2004). Removal of heavy metals from the environment by biosorption. Engineering in Life Sciences, 4(3), 219–232.

[9]. Goci, E., Droboniku, A., & Dilo, T. (2023). Advances in chitosan-based nanocomposites for environmental remediation: A review. Polymers, 15(4), 1024.

[10]. Gupta, V. K., Agarwal, S., & Saleh, T. A. (2016). Chromium removal by combining the magnetic properties of iron oxide with adsorption properties of carbon nanotubes. Water Research, 45(6), 2207–2212.

[11]. Jabeen, A., Kausar, A., Iqbal, M., & Bhatti, H. N. (2022). Chitosan-based composites for the removal of toxic heavy metals from industrial wastewater. Environmental Technology & Innovation, 26, 102378.

[12]. Karthik, R., Meenakshi, S., & Jegatha Narayanan, P. (2022). Adsorption studies of Pb(II) and Cd(II) ions from aqueous solutions using chitin extracted from fish scales. Bioresource Technology, 124, 448–455.

[13]. Khalid, N., Ahmad, S., Kiani, S. N., & Ahmed, J. (2000). Removal of lead from aqueous solutions using rice husk. Separation Science and Technology, 35(16), 2745–2772.

[14]. Krishna, R. H., & Swamy, A. V. V. S. (2012). Physico-chemical key parameters, Langmuir and Freundlich isotherm studies for the adsorption of divalent nickel onto powder of calcined brick. International Journal of Engineering Research and Development, 4(1), 29–38.

[15]. Kurita, K. (2020). Controlled functionalization of the polysaccharide chitin. Progress in Polymer Science, 26(9), 1921–1971.

[16]. Kurniawan, T. A., Chan, G. Y. S., Lo, W. H., & Babel, S. (2006). Physico-chemical treatment techniques for wastewater laden with heavy metals. Chemical Engineering Journal, 118(1–2), 83–98.

[17]. Mahmoud, M. E., Abdelfattah, A. M., & El-Gendi, A. (2023). Removal of Cr(III) and Ni(II) from wastewater using chitosan derived from fish waste. Chemical Engineering Research and Design, 189, 112–125.

[18]. Mahamallik, P., Saha, S., & Pal, A. (2021). Tetracycline degradation in aqueous solution by activated persulfate using modified chitosan nanocomposite. Journal of Environmental Management, 261, 110268.

[19]. Mousavi, S. M., & Seyedi, S. R. (2021). Adsorption of heavy metals from aqueous solutions using chitosan-based adsorbents: A systematic review. Desalination and Water Treatment, 213, 198–215.

[20]. Nanganoa, L. T., Ketcha, J. M., & Ndi, J. N. (2014). Kinetics and equilibrium studies of the adsorption of salicylic acid from aqueous solution by alluvial clay. Research Journal of Chemical Sciences, 4(5), 1–8.

[21]. Naswir, M., Arita, S., Marsi, M., & Salni, S. (2013). Utilization of zeolite to increase pH and adsorption phosphorus in peat soil. Journal of Environmental Science and Technology, 6, 152–159.

[22]. N'diaye, A. D., Kankou, M. S. A., & Bollahi, M. A. (2022). Adsorption of heavy metals onto chitosan from rice bran: Isotherm and kinetic studies. Journal of Materials and Environmental Science, 13(1), 1–12.

[23]. Ngah, W. S. W., & Fatinathan, S. (2010). Adsorption of Cu(II) ions in aqueous solutions using chitosan beads, chitosan-GLA beads and chitosan-alginate beads. Chemical Engineering Journal, 143(1–3), 62–72.

[24]. Okpaegbe, U. C., Milam, C., & Maitera, O. N. (2021). Removal of Cd(II) and Mn(II) ions from aqueous solution using chitosan and its derivatives from fish scale "Giwan Ruwa" (*Lates niloticus*). International Journal of Progressive Research in Science and Engineering, 2(8), 116–121.
[25]. Reddad, Z., Gerente, C., Andres, Y., & Le Cloirec, P. (2002). Adsorption of several metal ions onto a low-cost biosorbent: Kinetic and equilibrium studies. Environmental Science & Technology, 36(9), 2067–2073.
[26]. Rinaudo, M. (2018). Chitin and chitosan: Properties and applications. Progress in Polymer Science, 31(7), 603–632.
[27]. Tan, X., Liu, Y., Zeng, G., Wang, X., Hu, X., Gu, Y., & Yang, Z. (2012). Application of biochar for the removal of pollutants from aqueous solutions. Chemosphere, 125, 70–85.
[28]. Yadav, M., Goswami, P., Paritosh, K., Kumar, M., Pareek, N., & Vivekanand, V. (2019). Seafood waste: A source for preparation of commercially employable chitin/chitosan materials. Bioresources and Bioprocessing, 6(1), 8